Sensor and Simulation Notes

Note 89

June 1969

Waveforms Near a Cylindrical Antenna

by

R. W. Latham and K. S. H. Lee

Northrop Corporate Laboratories
Pasadena, California

Abstract

The waveforms of the magnetic field are calculated and graphed at observation points close to, as well as far away from, an infinite cylindrical antenna excited by a step-function voltage across a circumferential gap of infinitesimal width. Analytical expressions for the early time and the late time behavior of the field are also derived. Precise criteria are given concerning the validity of some previous results obtained by performing an inverse Laplace transform on the time-harmonic far-field expression.

I. Introduction

Recently we have presented some quantitative results on the radiation field of an infinite cylindrical antenna, loaded with either finite or zero resistance per unit length and excited by a step-function voltage across a delta gap.[1,2] The method used in the previous calculations is first to make the far-zone approximation to the time-harmonic field and then to invert this far-field expression to the time domain. Although the results obtained via this method are, to be sure, correct for distances very far away from the antenna and for not too long an observation time, it is not clear precisely where and when the results do not hold. To settle this question we have to look for an expression for the field valid everywhere and for all time, and from this expression we can then deduce, analytically or numerically, some precise criteria for the validity of the previous results. This is one objective of this note.

The second objective of this note is to present some new results on the time behavior of the field near the antenna. These results should be valuable in the present development of an airborne EMP simulator.

One aspect of the present problem has been considered by Wu[3]; that is, he calculated the total current on an infinite cylindrical antenna excited by a step-function across a delta gap. Later, Morgan re-derived Wu's expression for the current by a different method.[4] Independently, Brundell[5] studied the same problem with a treatment of the field included; however, he gave no quantitative results. The approach we shall use is slightly different from Brundell's, but much simpler. We shall numerically evaluate some derived formulas for the field and present some quantitative results in graphical form.

In Section II, we begin with a previously derived expression for the time-harmonic magnetic field and proceed to take its inverse Laplace transform for a step-function excitation. After several transformations of variables we arrive at a contour integral. This contour integral is then deformed, in Section III, into two different representations by a real integral, one of which is suitable for numerical computation. In Section IV, some limiting forms of the solution for small and large times are given, together with a few concluding remarks.

II. Formulation

The time-harmonic magnetic field $\widetilde{H}_\phi$ of a perfectly conducting, infinite cylindrical antenna of radius a and having $\widetilde{E}_z = -\widetilde{V}\delta(z)$ on its surface is given by[2]

$$\widetilde{H}_\phi(\rho,z) = \frac{ik\widetilde{V}}{2\pi Z_o} \int_{-\infty}^{\infty} \frac{H_1^{(1)}(\rho(k^2-\zeta^2)^{1/2})}{H_o^{(1)}(a(k^2-\zeta^2)^{1/2})} \frac{e^{i\zeta z}}{(k^2-\zeta^2)^{1/2}} d\zeta \quad . \tag{1}$$

The geometry and notation of the present problem are the same as in references 1 and 2, and are depicted in Fig. 1.

Let $p = -ik$ and $\widetilde{V} = v_o/(pc)$, i.e., the excitation is a step function of voltage v_o. Then, the inverse Laplace transform of (1) gives

$$\frac{Z_o H_\phi(\rho,z,t)}{v_o} = \frac{1}{2\pi i}\int_{C_p} e^{pct}\, dp \cdot \frac{1}{2\pi}\int_{-\infty}^{\infty} \frac{K_1(\nu\rho)}{\nu K_o(\nu a)} e^{i\zeta z}\, d\zeta \quad , \tag{2}$$

where $\nu = (\zeta^2+p^2)^{1/2}$, the proper branch of which is defined in Fig. 2. In going from (1) to (2) we have used $(-\zeta^2-p^2)^{1/2} = i(\zeta^2+p^2)^{1/2}$, $H_o^{(1)}(ix) = -i(2/\pi)K_o(x)$, and $H_1^{(1)}(ix) = -(2/\pi)K_1(x)$. The paths of integration are shown in figures 2 and 3.

We now change the integral over ζ in equation (2) to that over ν. First, let us determine the path of integration C_ν in the ν-plane. Since $\zeta = (\nu^2-p^2)^{1/2}$, we must choose the branch of $(\nu^2-p^2)^{1/2}$ in the ν-plane such that along C_ν we have

(i) ζ to be real in conformity with the path of the ζ-integral,

(ii) $\mathrm{Re}\,\nu \geq 0$ to guarantee damped waves for $\rho \to \infty$,

(iii) $\mathrm{Im}\,\zeta > 0$ for $z > 0$, and $\mathrm{Im}\,\zeta < 0$ for $z < 0$ so that the waves are damped for $|z| \to \infty$.

Now we write

$$\zeta = \sqrt{(\nu_1 + i\nu_2)^2 - (p_1 + ip_2)^2}$$

$$= \sqrt{(\nu_1^2 - \nu_2^2 - p_1^2 + p_2^2) + 2i(\nu_1\nu_2 - p_1p_2)}$$

To make ζ real along C_ν we must choose C_ν such that

$$\nu_1\nu_2 = p_1p_2 \tag{3a}$$

and

$$\nu_1^2 - \nu_2^2 - p_1^2 + p_2^2 \geq 0 \quad . \tag{3b}$$

Thus, C_ν must run alongside the part of hyperbolas (3a) where (3b) is satisfied and $\nu_1 \geq 0$. Since ζ is positive real on one part of C_ν and negative real on the other part of C_ν (that is, the phase of ζ differs by π in going from one part of the path to the other), there must be a branch cut running between the two parts of C_ν . Hence, we arrive at Fig. 4 without the arrows, and the direction of C_ν is still to be determined.

To determine the direction of C_ν we define the two branches of $\sqrt{\nu^2 - p^2}$ as follows. The first branch is defined so that $\zeta = ip$ at $\nu = 0$ and the second branch is defined so that $\zeta = -ip$ at $\nu = 0$. Clearly, the first Riemann sheet maps into the upper ζ-plane and the second sheet maps into the lower ζ-plane. Then, in accordance with the condition (iii) we use the first branch for $z > 0$ and the second branch for $z < 0$. It is not difficult to see that the path C_ν depicted in Fig. 4 actually corresponds to a path slightly displaced from the real ζ-axis into the upper ζ-plane. A path slightly displaced from the real ζ-axis into the lower ζ-plane (for $z < 0$) will transform into C'_ν on the second Riemann sheet with direction opposite to C_ν.

Under the transform $\zeta = \sqrt{\nu^2 - p^2}$ we now can write (2) as follows:

$$\frac{Z_o H_\phi}{V_o} = \frac{1}{2\pi i} \int_{C_p} e^{pct}\, dp \, \frac{1}{2\pi} \int_{C_\nu} \frac{K_1(\nu\rho)}{K_o(\nu a)} \frac{e^{i\sqrt{\nu^2 - p^2}z}}{\sqrt{\nu^2 - p^2}}\, d\nu\ , \qquad z > 0 \tag{3}$$

Since on the first Riemann sheet $\sqrt{\nu^2 - p^2} \to \pm\,\nu$ as $|\nu| \to \infty$ in the first and fourth quadrant of the ν-plane respectively, and since $K_o(\nu a)$ has no zeros for $|\arg \nu| \le \pi/2$, we can deform C_ν into Γ_ν as shown in Fig. 4. Now the branch point $\nu = p$ always lies to the right of Γ_ν (that is to say, Γ_ν can be made independent of p) and, therefore, we can interchange the order of integration in (3) and obtain, with $\sqrt{\nu^2 - p^2} = i\sqrt{p^2 - \nu^2}$,

$$\frac{Z_o H_\phi}{V_o} = \frac{1}{2\pi i} \int_{\Gamma_\nu} \frac{K_1(\nu\rho)}{K_o(\nu a)}\, d\nu \cdot \frac{1}{2\pi i} \int_{C_p} \frac{e^{-\sqrt{p^2 - \nu^2}z}}{\sqrt{p^2 - \nu^2}}\, e^{pct}\, dp$$

$$= \frac{1}{2\pi i} \int_{\Gamma_\nu} \frac{K_1(\nu\rho)}{K_o(\nu a)}\, I_o(\nu\sqrt{(ct)^2 - z^2})\, d\nu\ , \qquad \text{for} \quad ct > z \tag{4}$$

$$= 0 \qquad\qquad \text{for} \quad ct < z$$

where we have used a well-known result for the inner integral.[6]

The integrand in (4) has no singularities to the right of Γ_ν (Fig. 5) and behaves as $\exp[-\nu(\rho - a - \sqrt{(ct)^2 - z^2})]$ as $|\nu| \to \infty$ in the right half plane. Thus, (4) gives

$$\frac{Z_o H_\phi}{v_o} = 0 \quad , \qquad \text{for} \quad ct < \sqrt{(\rho - a)^2 + z^2} \tag{5}$$

as it should.

III. Solution

If Γ_ν is deformed into the imaginary axis of the ν-plane (Fig. 5) we have, noting that the integral around the branch point $\nu = 0$ is zero,

$$\frac{Z_o H_\phi}{v_o} = \frac{1}{2\pi i} \int_{\Gamma_\nu} \frac{K_1(\nu\rho)}{K_o(\nu a)} I_o(\nu\tau) d\nu \qquad \tau = ((ct)^2 - z^2)^{1/2}$$

$$= \frac{1}{2\pi i} \int_{-i\infty}^{o} \frac{K_1(\nu\rho)}{K_o(\nu a)} I_o(\nu\tau) d\nu + \frac{1}{2\pi i} \int_{o}^{i\infty} \frac{K_1(\nu\rho)}{K_o(\nu a)} I_o(\nu\tau) d\nu \tag{6}$$

$$= \frac{1}{2\pi} \int_{-\infty}^{o} \frac{K_1(i\nu_2\rho)}{K_o(i\nu_2 a)} I_o(i\nu_2\tau) d\nu_2 + \frac{1}{2\pi} \int_{o}^{\infty} \frac{K_1(i\nu_2\rho)}{K_o(i\nu_2 a)} I_o(i\nu_2\tau) d\nu_2$$

$$= -\frac{i}{2\pi} \int_{o}^{\infty} \frac{H_1^{(2)}(\nu_2\rho)}{H_o^{(2)}(\nu_2 a)} J_o(\nu_2\tau) d\nu_2 + \frac{i}{2\pi} \int_{o}^{\infty} \frac{H_1^{(1)}(\nu_2\rho)}{H_o^{(1)}(\nu_2 a)} J_o(\nu_2\tau) d\nu_2$$

$$= \frac{1}{\pi} \int_{o}^{\infty} \frac{J_1(\nu_2\rho) Y_o(\nu_2 a) - J_o(\nu_2 a) Y_1(\nu_2\rho)}{J_o^2(\nu_2 a) + Y_o^2(\nu_2 a)} J_o(\nu_2((ct)^2 - z^2)^{1/2}) d\nu_2 . \tag{7}$$

Setting $\rho = a$ in (7) we find that the total current $I(z,t)$ is given by

$$I(z,t) = 2\pi a H_\phi = \frac{4v_o}{\pi Z_o} \int_{o}^{\infty} \frac{J_o(\nu_2((ct)^2 - z^2)^{1/2})}{J_o^2(\nu_2 a) + Y_o^2(\nu_2 a)} \frac{d\nu_2}{\nu_2} \tag{8}$$

which is identical to Wu's expression.[3]

To obtain a form suitable for numerical integration we proceed as follows.

First, we substitute[7] $\pi i I_o(\nu\tau) = K_o(\nu\tau) - K_o(\nu\tau e^{i\pi})$ and $\pi i I_o(\nu\tau) = K_o(\nu\tau e^{-i\pi}) - K_o(\nu\tau)$ into the first and second integrals in (6) respectively and obtain

$$\frac{Z_o H_\phi}{V_o} = -\frac{1}{2\pi^2}\int_{-i\infty}^{o} \frac{K_1(\nu\rho)}{K_o(\nu a)}\left[K_o(\nu\tau) - K_o(\nu\tau e^{i\pi})\right]d\nu$$

$$-\frac{1}{2\pi^2}\int_{o}^{i\infty} \frac{K_1(\nu\rho)}{K_o(\nu a)}\left[K_o(\nu\tau e^{-i\pi}) - K_o(\nu\tau)\right]d\nu$$

$$= \frac{1}{2\pi^2}\int_{-i\infty}^{o} \frac{K_1(\nu\rho)}{K_o(\nu a)} K_o(\nu\tau e^{i\pi})d\nu - \frac{1}{2\pi^2}\int_{o}^{i\infty} \frac{K_1(\nu\rho)}{K_o(\nu a)} K_o(\nu\tau e^{-i\pi})d\nu$$

$$-\frac{1}{2\pi^2}\int_{-i\infty}^{o} \frac{K_1(\nu\rho)}{K_o(\nu a)} K_o(\nu\tau)d\nu + \frac{1}{2\pi^2}\int_{o}^{i\infty} \frac{K_1(\nu\rho)}{K_o(\nu a)} K_o(\nu\tau)d\nu \qquad (9)$$

We now deform the integration path of the first integral into $C_3 + L_-$, that of the second integral into $C_2 + L_+$, and those of the last two integrals into the positive real axis (Fig. 5). From the asymptotic forms of K_o and K_1 it is easily seen that respective integrals over the infinite quarter circles C_1, C_2, C_3 and C_4 vanish for $\tau > \rho - a$. By making use of the formula[7]

$$K_\mu(ze^{m\pi i}) = e^{-m\pi i} K_\mu(z) - \pi i \frac{\sin m\mu\pi}{\sin \mu\pi} I_\mu(z)$$

the integrals over L_-, L_+ and the real positive axis become

$$\frac{Z_o H_\phi}{V_o} = -\frac{1}{2\pi^2}\int_o^\infty \frac{K_1(\nu_1\rho) - \pi i I_1(\nu_1\rho)}{K_o(\nu_1 a) + \pi i I_o(\nu_1 a)} K_o(\nu_1\tau)d\nu_1$$

$$-\frac{1}{2\pi^2}\int_o^\infty \frac{K_1(\nu_1\rho) + \pi i I_1(\nu_1\rho)}{K_o(\nu_1 a) - \pi i I_o(\nu_1 a)} K_o(\nu_1\tau)d\nu_1$$

$$+\frac{1}{\pi^2}\int_o^\infty \frac{K_1(\nu_1\rho)}{K_o(\nu_1 a)} K_o(\nu_1\tau)d\nu_1$$

$$= \int_o^\infty \frac{I_o(\nu_1 a)[I_o(\nu_1 a)K_1(\nu_1\rho) + I_1(\nu_1\rho)K_o(\nu_1 a)]}{K_o(\nu_1 a)[K_o^2(\nu_1 a) + \pi^2 I_o^2(\nu_1 a)]} K_o(\nu_1\tau)d\nu_1 \text{ , for } \tau > \rho - a \qquad (10)$$

Writing $u = \nu_1 a$ and multiplying both sides by r we finally arrive at the dimensionless form

$$\frac{rZ_o H_\phi}{V_o} = \frac{r}{a}\int_o^\infty \frac{I_o(u)[I_o(u)K_1(u\ \rho/a) + K_o(u)I_1(u\ \rho/a)]}{K_o(u)[K_o^2(u) + \pi^2 I_o^2(u)]} K_o(u\ \tau/a)du \quad , \qquad (11)$$

$$\text{for} \quad ct > ((\rho - a)^2 + z^2)^{1/2}$$

This integral was numerically evaluated as function of T for several values of r and θ , where T is defined by

$$T = \frac{ct - ((\rho - a)^2 + z^2)^{1/2}}{a}$$

The results are presented in figures 6 through 13.

Setting $\rho = a$ in (11) and making use of the Wronskian relation among the modified Bessel functions we arrive at an alternative representation for the total current

$$I(z,t) = \frac{4v_o}{\pi Z_o} \int_o^\infty \frac{I_o(u) K_o(u\ \tau/a)}{K_o(u)[K_o^2(u) + \pi^2 I_o^2(u)]} \frac{du}{u}$$

which was used for numerical computation in Ref. 3.

IV. Remarks

It is expected that, for $\rho/a >> 1$ and for some interval of the observation time aT/c, equation (11) should reduce to equation (4) of Ref. 1. Since equation (11) is valid for $\tau > \rho - a$, the statement that $\rho/a >> 1$ also implies that $\tau/a >> 1$. Using the appropriate asymptotic forms for $I_1(u\,\rho/a)$, $K_1(u\,\rho/a)$ and $K_o(u\,\tau/a)$ in equation (11) we obtain

$$\frac{rZ_oH_\phi}{v_o} \sim \frac{r}{2\sqrt{\rho\tau}} \int_o^\infty \frac{I_o(u)}{K_o^2(u) + \pi^2 I_o^2(u)} \, e^{-u\left(\frac{\tau-\rho}{a}\right)} \frac{du}{u} \tag{12}$$

For observation time much smaller than ρ/c, i.e., for $T << \rho/a$, we have $ct - r << \rho$. Then

$$\tau = ((ct)^2 - z^2)^{1/2} = ([(ct - r) + r]^2 - z^2)^{1/2}$$

$$= (\rho^2 + 2r(ct - r) + (ct - r)^2)^{1/2}$$

$$\approx \rho + \frac{ct - r}{\sin\theta} \quad .$$

Insertion of this approximate expression of τ in (12) gives

$$\frac{rZ_oH_\phi}{v_o} \sim \frac{1}{2\sin\theta} \int_o^\infty \frac{I_o(u)}{K_o^2(u) + \pi^2 I_o^2(u)} \, e^{-u\left(\frac{ct - r}{a\sin\theta}\right)} \frac{du}{u} \tag{13}$$

which is identical to the integral used in Ref. 1. Thus, the previous results are correct if $\rho/a >> 1$ and $T << \rho/a$.

The curves labelled "$r/a \geq 10^4$" in figures 6 through 13 correspond to those obtained in Ref. 1. It appears that there is a difference between them in the early times. This apparent discrepancy is due to two different definitions of T. Let T_{old} denote the T used in Ref. 1. Then, for $\rho/a >> 1$

$$T = \frac{ct - ((\rho - a)^2 + z^2)^{1/2}}{a} \sim \frac{ct - (r - a)}{a} + \sin\theta - 1$$

$$= T_{old} - (1 - \sin\theta) \quad .$$

This equation accounts for the difference just mentioned.

Next, we shall deduce the limiting forms of equation (11) for large T and small T. From the definition of τ, i.e.,

$$\frac{\tau}{a} = \frac{((ct)^2 - z^2)^{1/2}}{a} = \left\{T^2 + 2T\left(\left(\frac{\rho}{a} - 1\right)^2 + \left(\frac{z}{a}\right)^2\right)^{1/2} + \left(\frac{\rho}{a} - 1\right)^2\right\}^{1/2} \quad ,$$

we see that $\tau/a \to \infty$ as $T \to \infty$, and that $\tau/a \to \rho/a - 1$ as $T \to 0$.

<u>Late time behavior of rZ_oH_ϕ/v_o</u>

Substituting

$$K_o(u\,\tau/a) = \int_1^\infty \frac{e^{-xu\,\tau/a}}{\sqrt{x^2 - 1}}\,dx$$

into equation (11) and interchanging the order of integration we have

$$\frac{rZ_oH_\phi}{v_o} = \frac{r}{a}\int_1^\infty \frac{dx}{\sqrt{x^2-1}}\int_0^\infty \frac{I_o(u)[I_o(u)K_1(u\,\rho/a) + K_o(u)I_1(u\,\rho/a)]}{K_o(u)[K_o^2(u) + \pi^2 I_o^2(u)]}\, e^{-ux\,\tau/a}\, du \;. \quad (14)$$

For large $x\,\tau/a$ the inner integral can be evaluated asymptotically in the same way as described in Ref. 1. Thus, (14) becomes

$$\frac{rZ_oH_\phi}{v_o} \sim \frac{1}{2\sin\theta}\int_1^\infty \frac{1}{\sqrt{x^2-1}}\,\frac{dx}{[\ln\frac{2\tau}{\Gamma a} + \ln x]^2} \qquad (\text{as} \quad \tau/a \to \infty)$$

$$= \frac{1}{2\sin\theta}\int_1^\infty \frac{d(\ln x)}{[\ln\frac{2\tau}{\Gamma a} + \ln x]^2}\,(1 - \frac{1}{x^2})^{-1/2}$$

$$\sim \frac{1}{2\sin\theta}\,\frac{1}{\ln(\frac{2\tau}{\Gamma a})} \quad , \qquad \text{as} \quad \tau/a \to \infty \qquad (15)$$

where $\Gamma = 1.7810\cdots$. It is to be noted that the asymptotic formula (15) was derived under the condition $\rho/a < \tau/a \to \infty$. For $T > 100$, one can use (15) to extend the curves, except the ones labelled "$r/a \geq 10^4$," in figures 10 through 13, since the difference between the results calculated by (15) and those obtained by numerically computing equation (11) is less than 3% for $T \geq 100$.

Early time behavior of rZ_oH_ϕ/v_o

Let $\tau/a - \rho/a + 1 = \varepsilon$. We wish to examine the limit of rZ_oH_ϕ/v_o as $\varepsilon \to 0$. Following the same procedure as in Ref. 1 we break equation (11) into two parts, viz.

$$\frac{rZ_oH_\phi}{v_o} = \frac{r}{a}\int_0^\delta (\cdots)du + \frac{r}{a}\int_\delta^\infty (\cdots)du = I_1 + I_2 \qquad ,$$

where δ is chosen in such a way that in evaluating I_2 one can use the asymptotic forms for the modified Bessel functions. Thus

$$I_2 \sim \frac{1}{\pi\sqrt{2\pi}} \frac{r}{\sqrt{\rho\tau}} \int_{\delta}^{\infty} \{e^{-u(\rho - a)/a} + e^{u(\rho - a)/a}\} \frac{e^{-u\varepsilon - u(\rho - a)/a}}{\sqrt{u}} du \quad . \tag{16}$$

If $\rho > a$ and $(\rho - a)/a >> \varepsilon \to 0$, then (16) gives

$$I_2 \sim \frac{1}{\pi\sqrt{2}} \frac{r}{\sqrt{\rho(\rho - a)}} \frac{1}{\sqrt{\varepsilon}} \quad . \tag{17a}$$

If $\rho = a$ and $\varepsilon \to 0$, then (16) gives

$$I_2 \sim \frac{\sqrt{2}}{\pi} (a^2 + z^2)^{\frac{1}{2}}((ct)^2 - z^2)^{-\frac{1}{2}} \quad . \tag{17b}$$

I_1 is easily seen to be negligible compared to I_2 when $\varepsilon \to 0$. The curves in figures 6 through 9 indeed have the behavior described by (17) for small T . Using (17b) one can immediately deduce that the total current $I(z,t)$ takes the form

$$I(z,t) \sim \frac{V_o}{Z_o} \frac{2\sqrt{2}\, a}{((ct)^2 - z^2)^{\frac{1}{2}}} \quad , \quad \text{as} \quad ct - z \to 0+ \quad .$$

Before concluding this note, two additional remarks are in order. Throughout this note we have treated exclusively the magnetic field H_ϕ , putting aside the non-vanishing components E_r and E_θ of the electric field. Of course, E_r and E_θ are obtainable from H_ϕ via Maxwell's equations; but an extra integration over time is required, thus making E_r and E_θ expressible in terms of double integrals. Very far away from the antenna, however, we have—$E_\theta = Z_o H_\phi$, i.e., E_θ and $Z_o H_\phi$ have identical waveforms. The reason that H_ϕ can be expressed as a single integral is that we have considered a step-function excitation which allows one integral of the double integral (i.e., the inner integral of (4)) to be evaluated explicitly. The second remark is that although we have treated an infinite antenna in this note, the results are still valid for an antenna of total length $2h$ if the observation time $aT/c < h/c + (R_2 - R_1)/c$, R_1 and R_2 being respectively the distance from the observation point to the excitation point and to the nearer end of the antenna.

References

1. R. W. Latham and K. S. H. Lee, Sensor and Simulation Note 73, "Pulse radiation and synthesis by an infinite cylindrical antenna," February 1969.
2. R. W. Latham and K. S. H. Lee, Sensor and Simulation Note 83, "Radiation of an infinite cylindrical antenna with uniform resistive loading," April 1969.
3. T. T. Wu, "Transient response of a dipole antenna," J. Math. Phys., Vol. 2, p. 892, 1961.
4. S. P. Morgan, "Transient response of a dipole antenna," J. Math. Phys., Vol. 3, p. 564, 1962.
5. Per-Olof Brundell, "Transient electromagnetic waves around a cylindrical transmitting antenna," Ericsson Technics, Sweden, Vol. 16, No. 1, pp. 137-162, 1960.
6. W. Magnus and F. Oberhettinger, Functions of Mathematical Physics, Chelsea Publishing Col, New York, p. 134, 1954.
7. G. N. Watson, Theory of Bessel Functions, Cambridge University Press, Cambridge, Second Edition, p. 80, 1944.

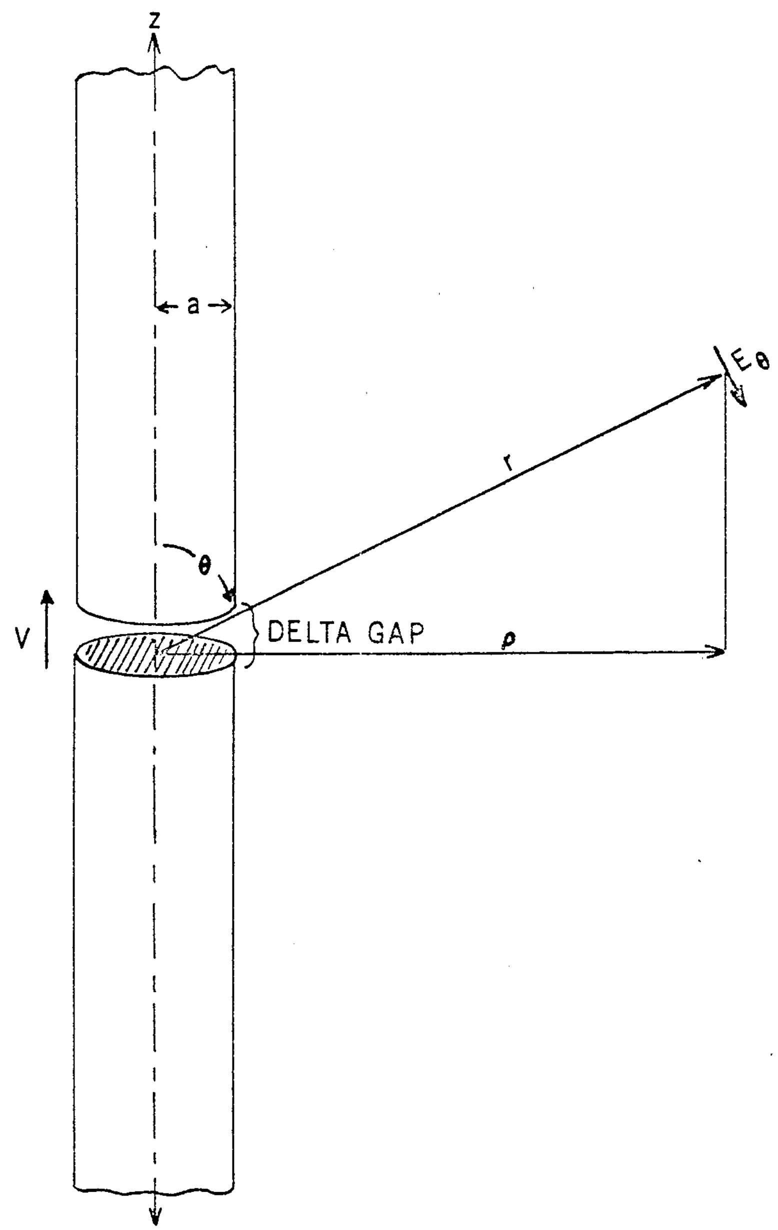

Figure 1. Infinite cylindrical antenna with a gap generator.

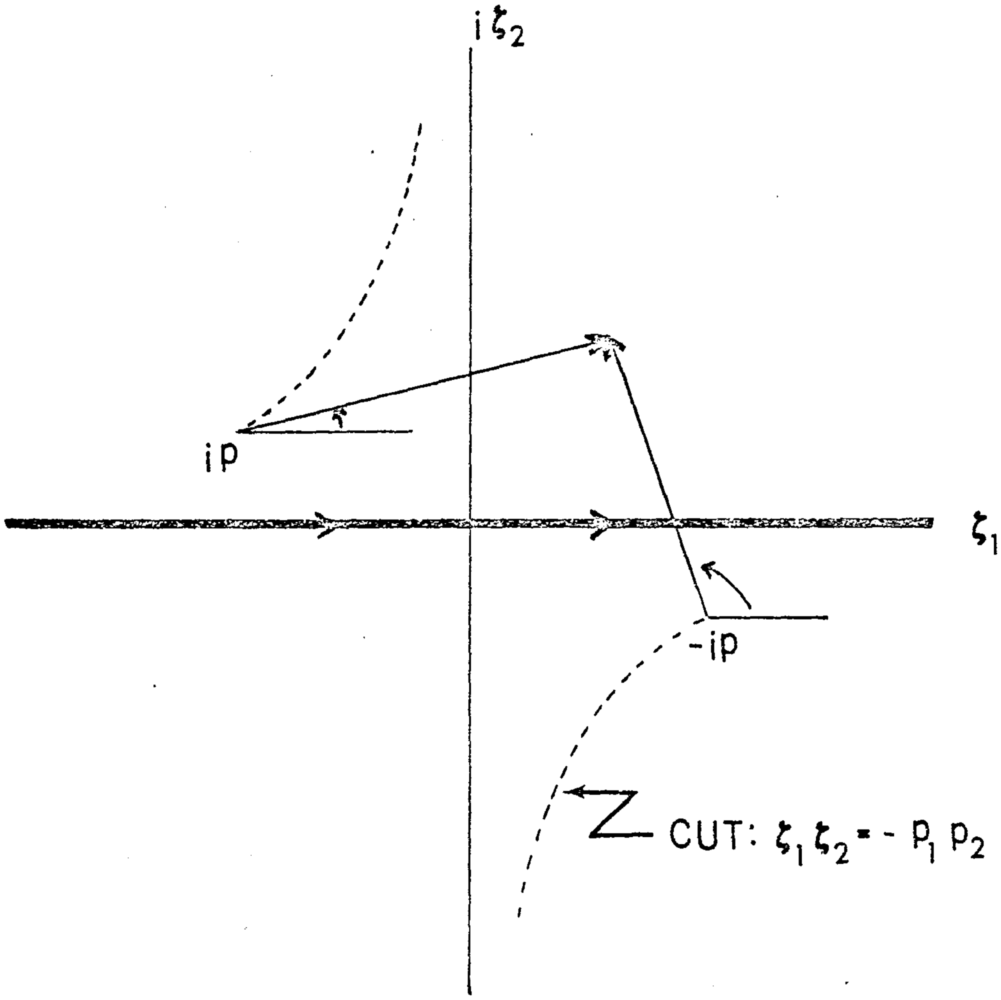

Figure 2. Branch of $\nu = \sqrt{\zeta^2 + p^2}$: $\nu = p$ at $\zeta = 0$.

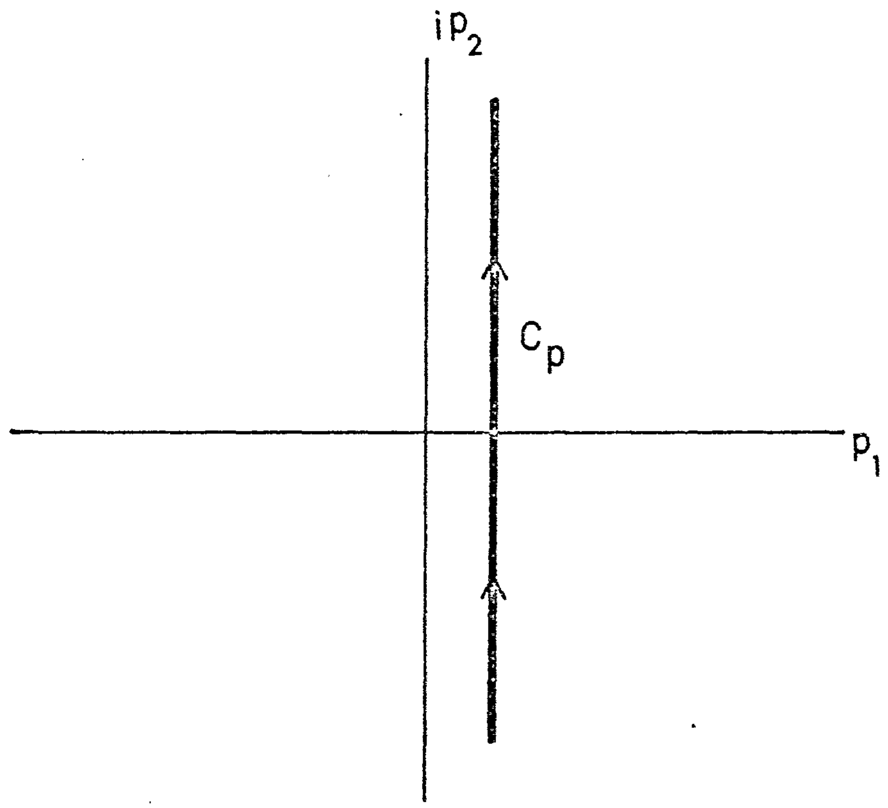

Figure 3. Path of Integration

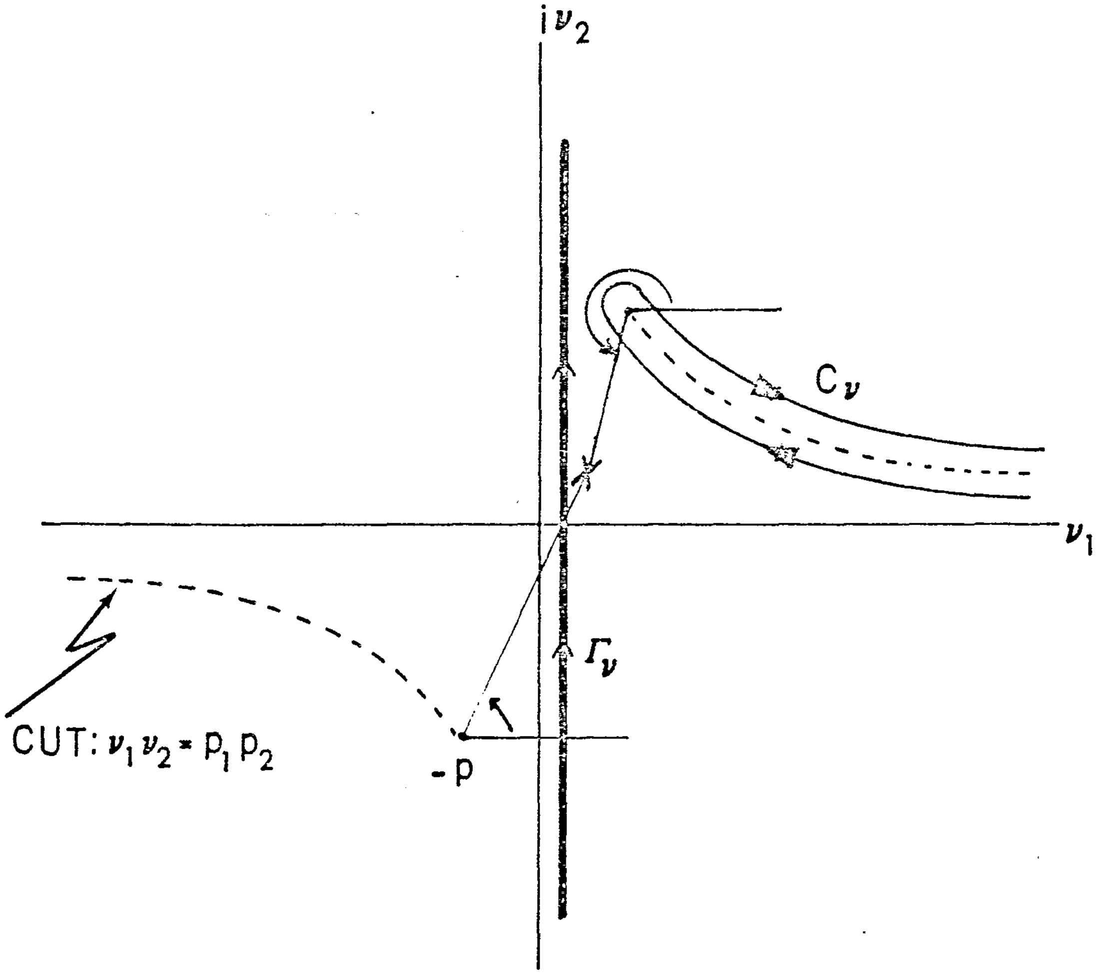

Figure 4. Branch of $\zeta = \sqrt{\nu^2 - p^2}$: $\zeta = ip$ at $\nu = 0$ if $z > 0$, and $\zeta = -ip$ at $\nu = 0$ if $z < 0$.

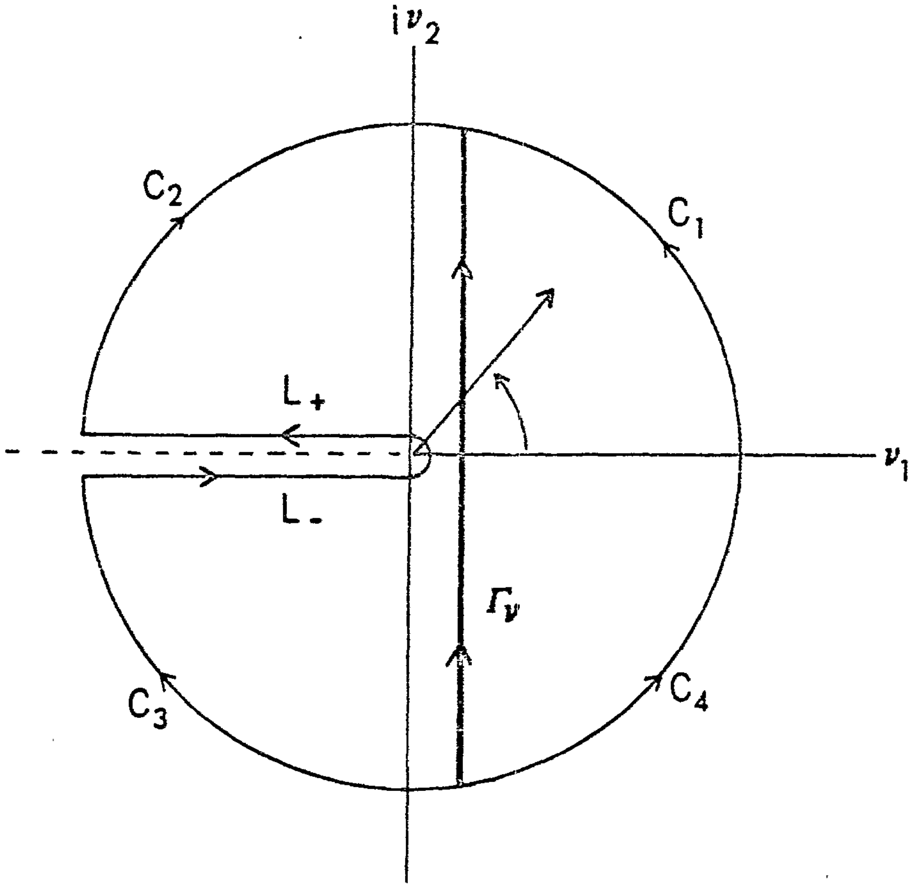

Figure 5. The branch where $|\arg \nu| < \pi$.

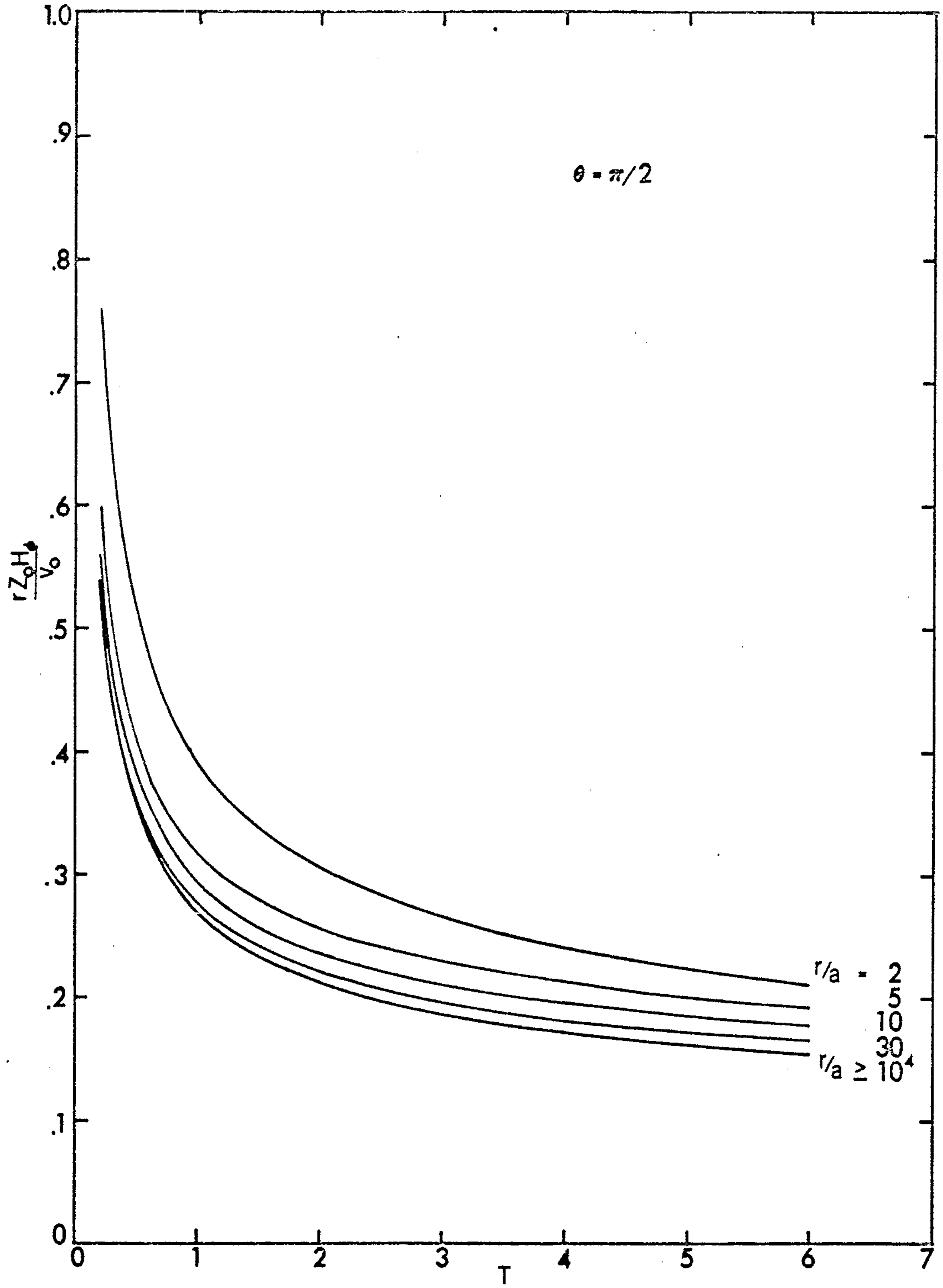

Figure 6. Magnetic-field waveforms for a step-function excitation.

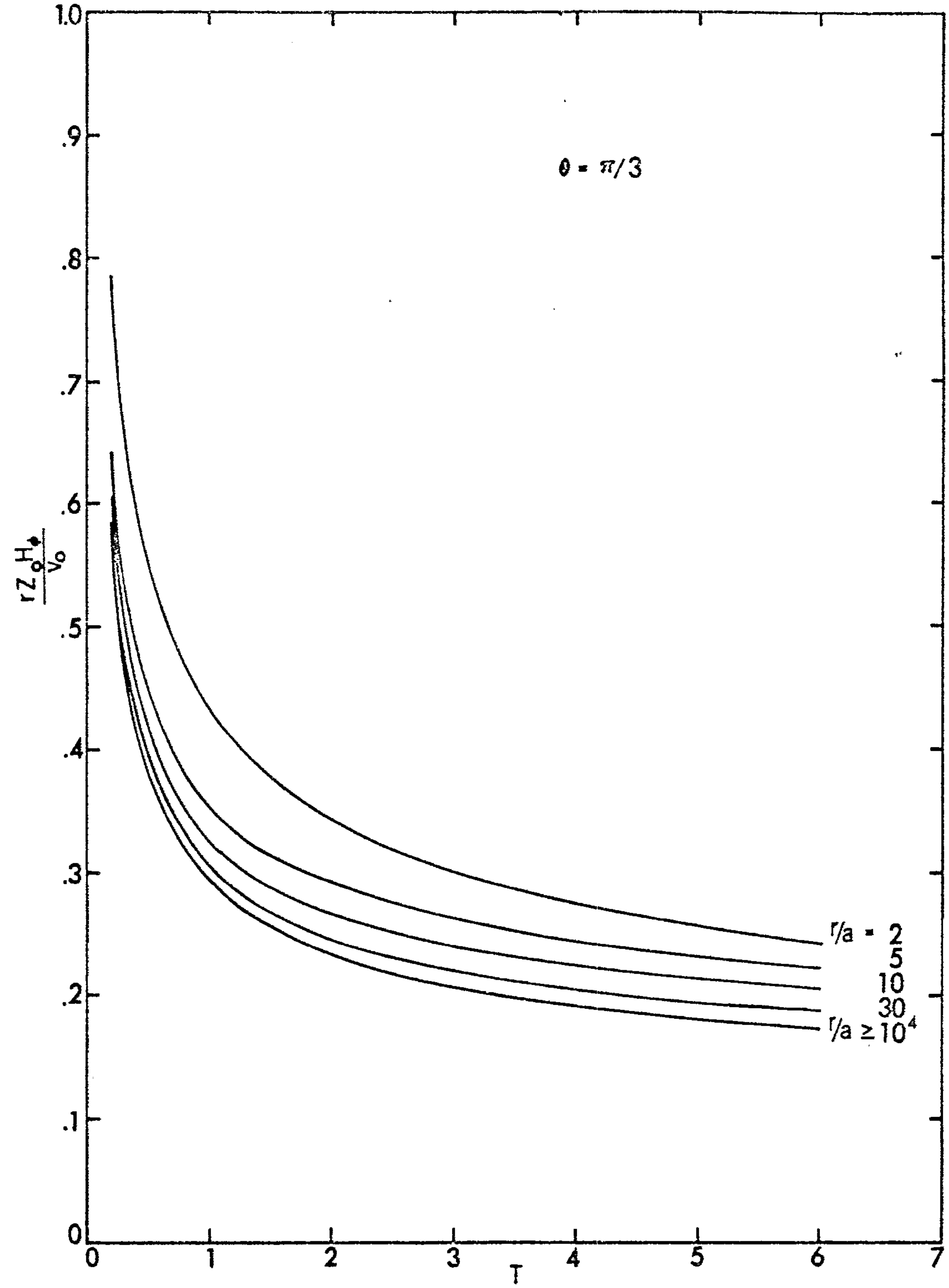

Figure 7. Magnetic-field waveforms for a step-function excitation.

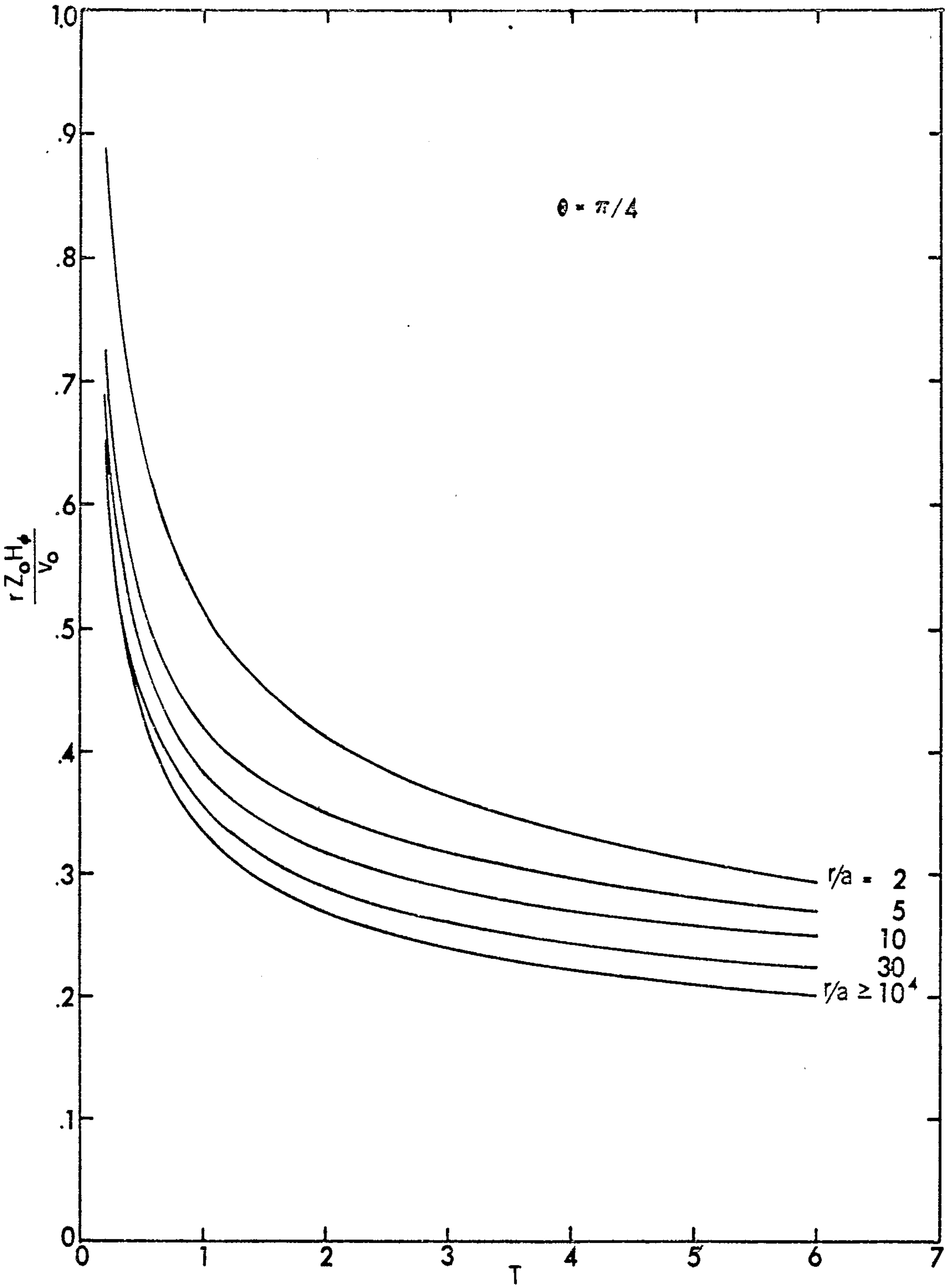

Figure 8. Magnetic-field waveforms for a step-function excitation.

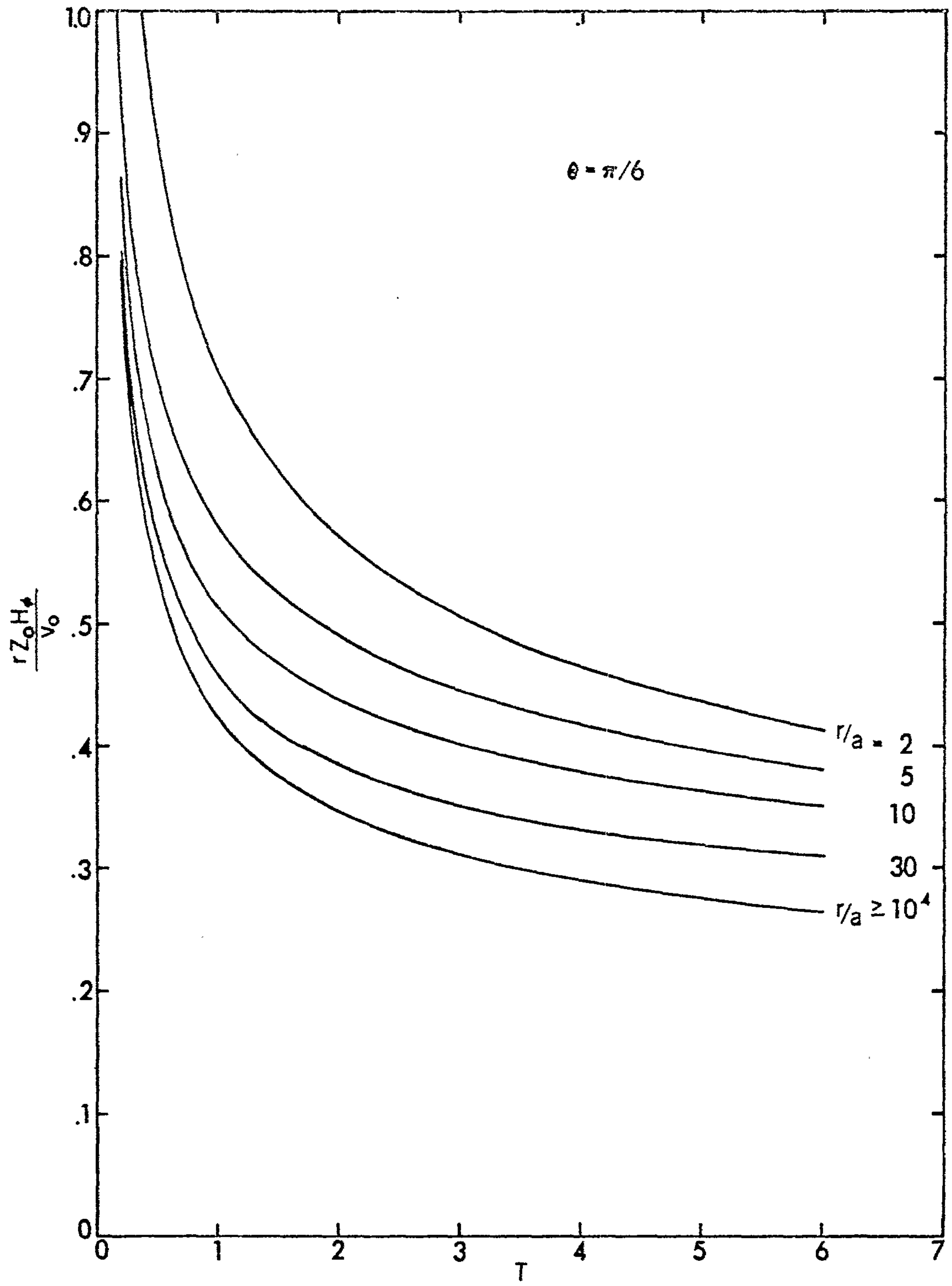

Figure 9. Magnetic-field waveforms for a step-function excitation.

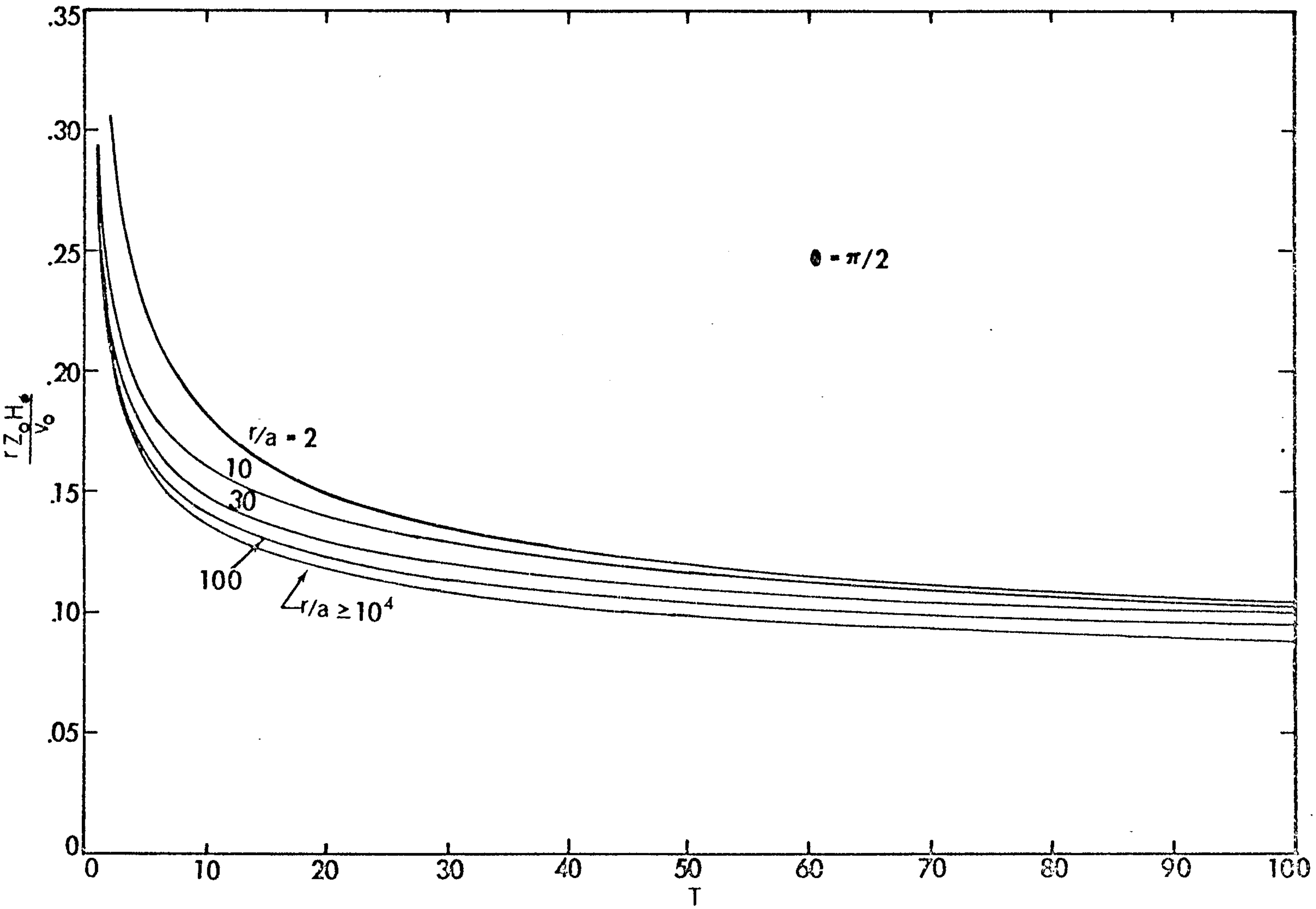

Figure 10. Magnetic-field waveforms for a step-function excitation.

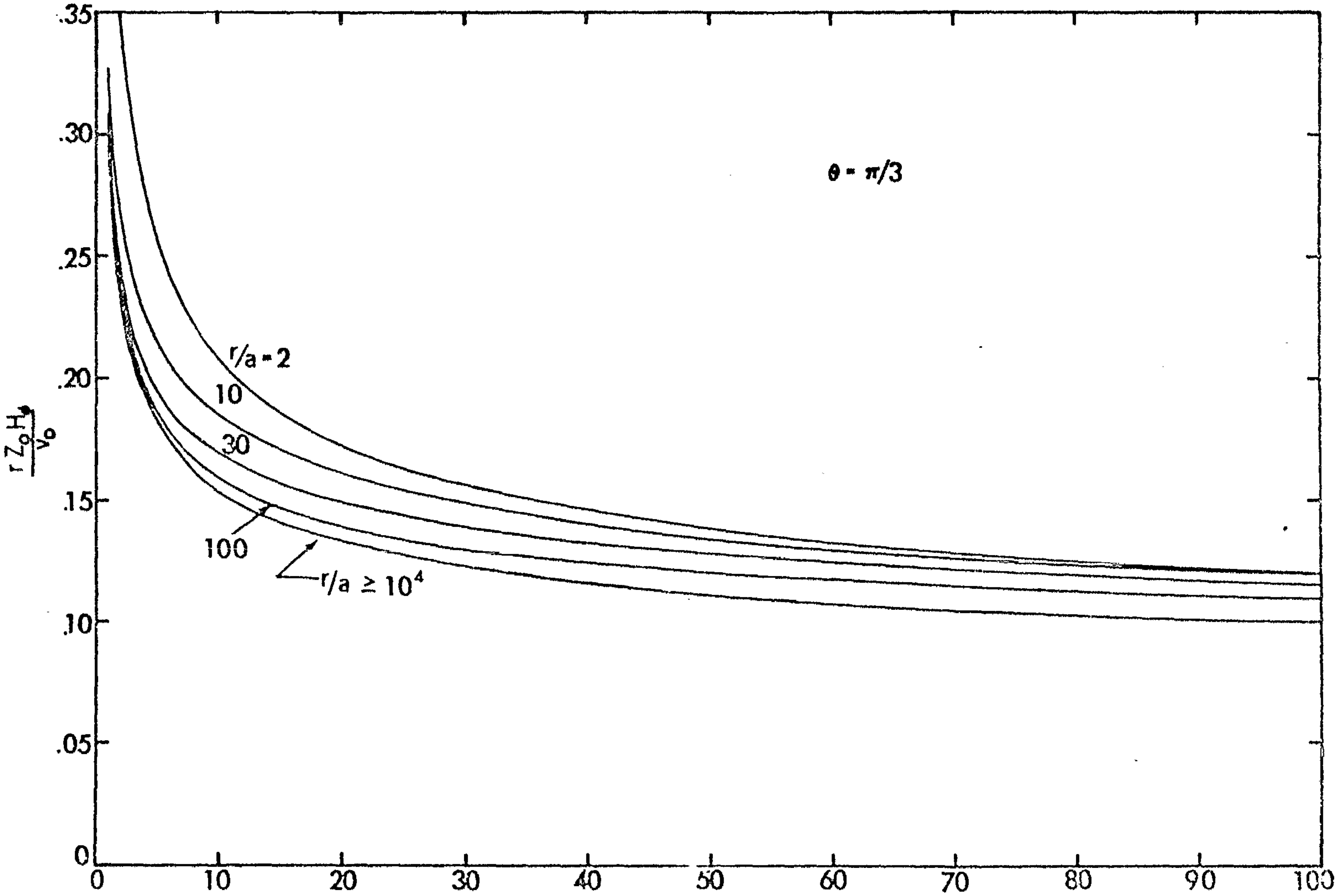

Figure 11. Magnetic-field waveforms for a step-function excitation.

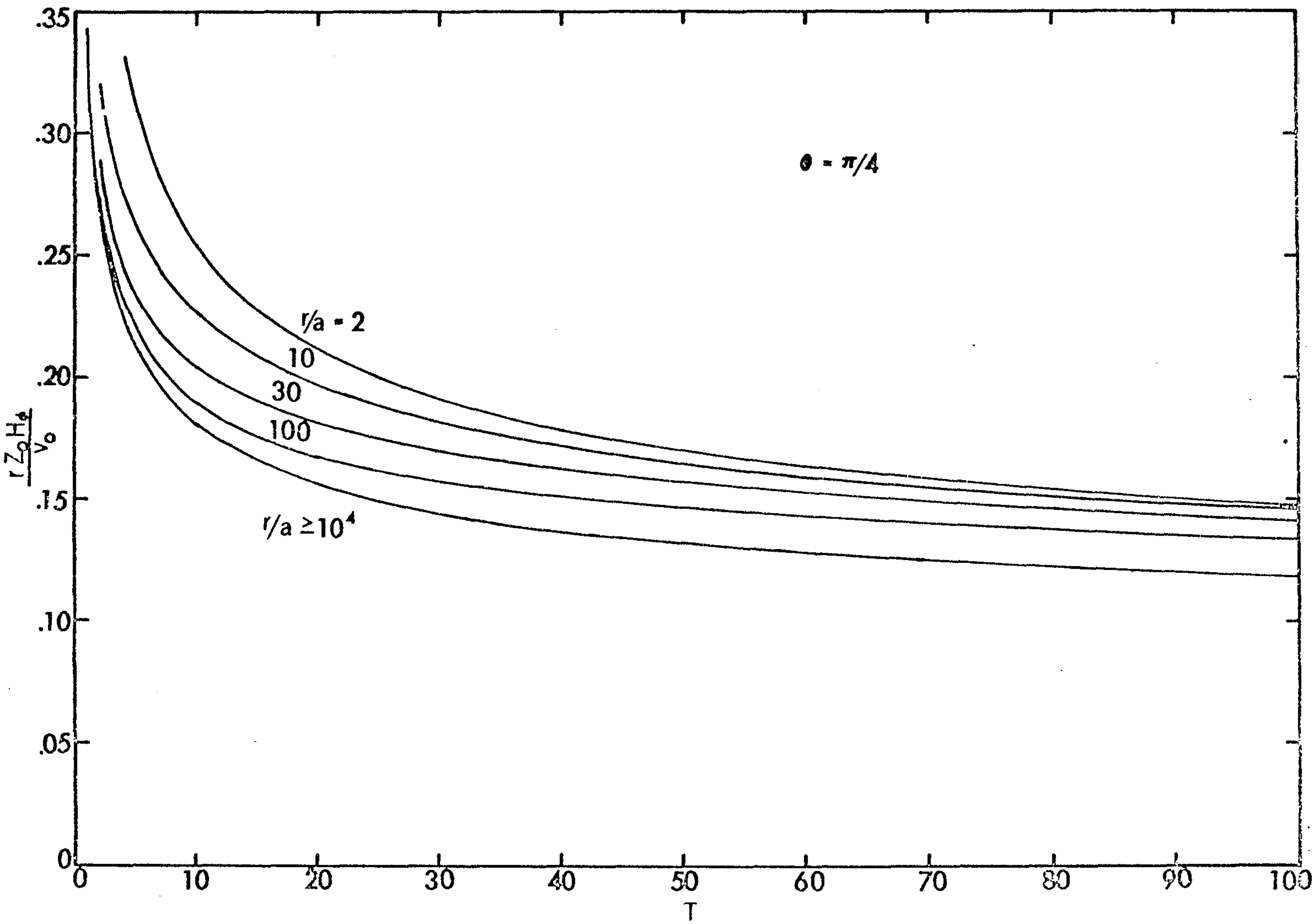

Figure 12. Magnetic-field waveforms for a step-function excitation.

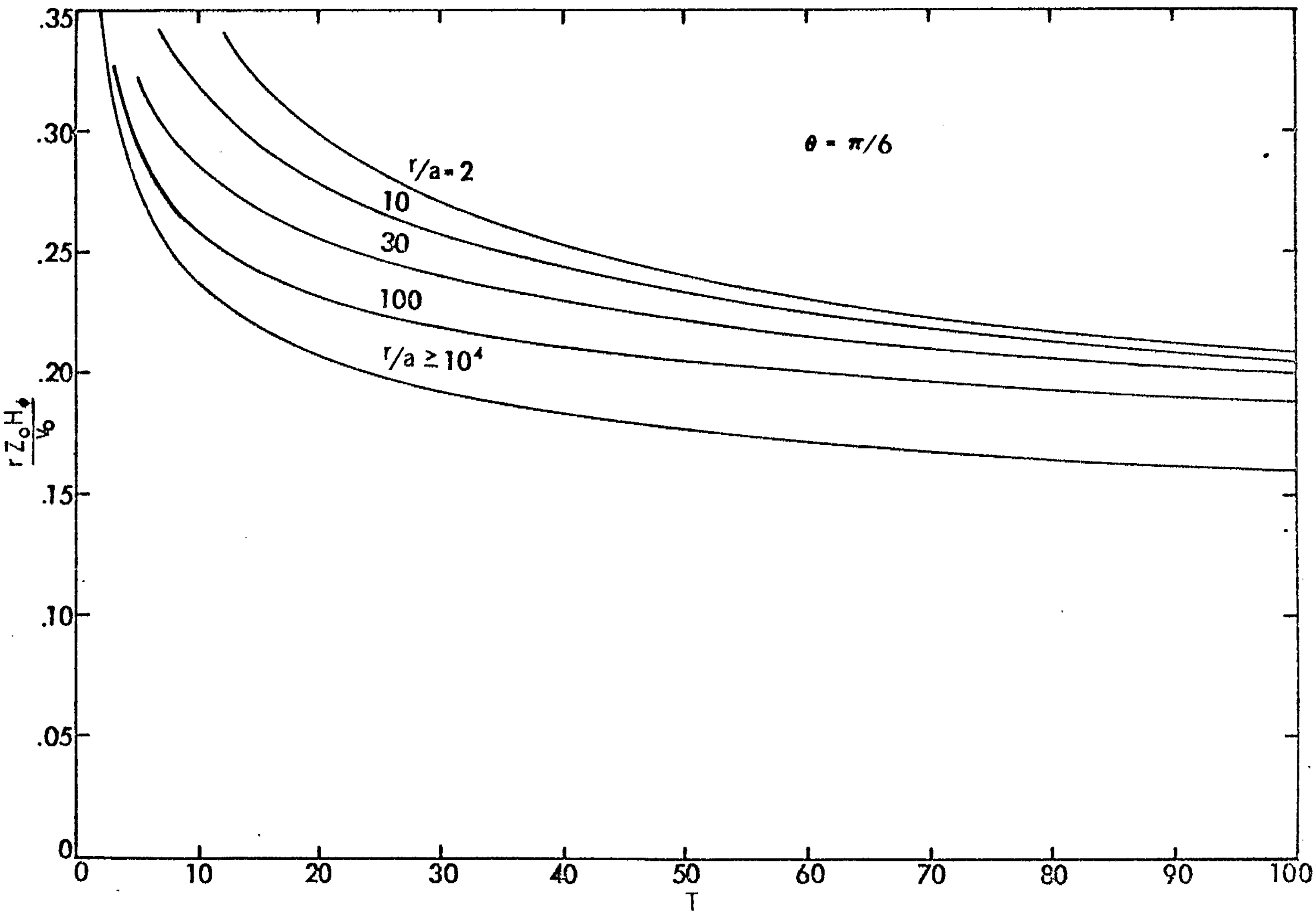

Figure 13. Magnetic-field waveforms for a step-function excitation.